Polymer Diffusion in Gel-Containing Poly(vinyl acetate-*co*-dibutyl maleate) Latex Films

J. P. S. Farinha,*,† Jun Wu,‡ Mitchell A. Winnik,*,‡ Rajeev Farwaha,§ and Jude Rademacher||

Centro de Química-Física Molecular, Instituto Superior Tecnico, 1049−001 Lisboa, Portugal, Department of Chemistry, University of Toronto, 80 St. George Street, Toronto, ON, M5S 3H6 Canada, Vinamul Polymers, 10 Finderne Avenue, Bridgewater, New Jersey 08807, and Research Center, ICI Paints, 16651 Sprague Road, Strongsville, Ohio 44136

Received January 26, 2005; Revised Manuscript Received March 11, 2005

ABSTRACT: Polymer interdiffusion in a poly(vinyl acetate-*co*-dibutyl maleate) [poly(VAc-*co*-DBM)] latex film containing ca. 50 wt % gel was studied by Förster resonance energy transfer (FRET). The latex particles were labeled either with an energy donor dye or with an acceptor dye. Films prepared from a mixture of donor- and acceptor-labeled particles exhibit nonexponential donor fluorescence decay profiles, which were analyzed in two distinct ways. In a first simplified approach, we calculated the fractional growth in the quantum efficiency of energy transfer f_m, from which we obtained an apparent diffusion coefficient, D_{app}, which decreases with increasing annealing time. In addition, we developed a new model for spherical diffusion that accounts for the presence of immobile gel nanodomains within the latex particles. We calculate the energy transfer from the donors in one particle to the acceptors in another, taking into account the concentration profile of the polymer arising from diffusion of the un-cross-linked chains through the gel nanodomains and across the particle boundary. By comparing simulated donor survival probabilities with experimental decay profiles, we obtained the polymer concentration profiles at the interface between particles and the corresponding mean cumulative diffusion coefficients $\langle D \rangle$, describing diffusion of the mobile polymer fraction, as a function of annealing time for different annealing temperatures. From the polymer concentration profile, we calculated the roughness of the initial interface (before any annealing) for gel containing latex particles. This value is much lower than that found for un-cross-linked samples. A comparison of the two methods of analysis shows that D_{app} values are up to three times larger than $\langle D \rangle$, but track the evolution of the "true" diffusion coefficient fairly well. From the temperature dependence of $\langle D \rangle$, we found an effective activation energy for diffusion of 39 kcal/mol.

Introduction

Polymer diffusion is an entropy-driven process by which macroscopic composition gradients relax in polymer systems.[1] It is usually referred to as self-diffusion when the matrix is composed of identical molecules to the test chain, and interdiffusion when the matrix is different.[1,2] Polymer diffusion has been a subject of intense interest for many years because it plays an important role in technological processes such as welding of polymer slabs, crack healing, sintering of polymer powders by compression molding, and formation and aging of latex films. In all these processes, polymer diffusion occurs across interfaces. Polymers are initially confined to opposite sides of the interface and diffusion across the interface generates entanglements, which increases the strength of adhesion. The thermodynamic interactions between the polymers govern the rate at which the macroscopic composition gradients relax and the width of the interface between the two constituents.[3] The properties of a system's interface, such as resistance to fracture, are strongly dependent on both of these quantities.[4]

For a polymer with an average molecular weight larger than the entanglement molecular weight (M_e), the diffusion mechanism can be described by combining reptation with segmental motion.[5,6] Four regimes are predicted theoretically for the dynamics of such a chain:[5,7,8] At times shorter than the entanglement relaxation time,τ_e, relaxation of segments within the entanglement length occurs. In this case the mean square displacement of the segments is smaller than the tube diameter, and the chains do not sense topological constraints. Between τ_e and the Rouse relaxation time, τ_R, the motion of a single segment becomes coordinated over the entire length of the chain, and its dynamics can be described by Rouse-like diffusion constrained inside the tube formed by the other chains. Between τ_R and the reptation time, τ_r, reptation dominates the chain motion. At longer times ($t > \tau_r$) the chain loses the memory of the original tube and continues the reptation motion in a new tube. Consequently, successive displacements are statistically independent, and over large time scales the dynamics of the polymer is described by the Fickian motion of its center-of-mass. With all these dynamic regimens, it is not surprising that the distribution function of polymer chains at the interface resulting from both reptation and segmental motion are rather complex for $t < \tau_r$.[7,8] However, for times longer than τ_r, the chain dynamics can be described by the diffusion of its center-of-mass, and the approximate concentration profiles across the interface can be obtained from the solution of Fick's diffusion equations.

Here, we are interested in interparticle polymer diffusion occurring during the aging process of latex films. When a latex film is cast from a dispersion, water evaporation and drying leads to the formation of a solid

* Corresponding authors. E-mail: (M.A.W.) mwinnik@chem.utoronto.ca; (J.P.S.F.) farinha@ist.utl.pt.
† Instituto Superior Tecnico.
‡ University of Toronto.
§ Vinamul Polymers.
|| ICI Paints.

10.1021/ma050167i CCC: $30.25
Published on Web 04/15/2005

film. For dispersions of surfactant-free particles with a narrow size distribution, this film has an ordered structure corresponding to densely close-packed polyhedral cells, as observed by transmission electron microscopy (TEM)[9,10] and freeze-fracture transmission electron microscopy (FF-TEM).[11,12] These cells are formed through deformation of the latex particles as the film dries.[13,14] The newly formed film is weak, because no polymer chains bridge the interface between adjacent cells. The mechanical strength of the film is improved as polymer molecules diffuse across the interface, leading to healing of the interface. Particle deformation can occur only if the system is at a temperature above the minimum film-forming temperature (MFT), which is close to the glass transition temperature (T_g) of the polymer in the presence of moisture. Polymer diffusion is usually very slow at the MFT. It occurs at a reasonable rate for chains of significant length only at temperatures at least 20−40 °C above T_g.

The interdiffusion process in latex films has been followed at the molecular level by small-angle neutron scattering (SANS), probing the growth of the radius of particles labeled with deuterium in a protonated matrix as the films are annealed.[15,16] Alternatively, the technique of nonradiative electronic energy transfer or Förster resonance energy transfer (FRET), offers several advantages: high sensitivity; easy labeling of the polymer with the required dyes; less interference in the polymer intrinsic properties. This is a quantitative technique based on dynamic fluorescence measurements. In a FRET experiment, one mixes two essentially identical types of latex particles in dispersion prior to film formation. Both types of latex particles are covalently labeled with about 1 mol % of dye, one with a fluorescent dye that can act as an electronic energy donor and the other with a corresponding acceptor dye.[17,18] The donor dye is then selectively excited and can subsequently fluoresce, or if there is a nearby acceptor dye, it can transfer energy to the acceptor dye via a resonant coupling of the transition dipoles.

When a dispersion containing donor- and acceptor-labeled particles dries to form a film, initially the donors and the acceptors are located in different particles, with FRET occurring only to a small extent across the particle boundaries. Annealing of the film at temperatures higher than the MFT promotes the interdiffusion of polymer chains between particles inducing the mixing of donors and acceptors and the consequent increase in the extent of FRET. The fluorescence decay curve of the donor reflects the increase of the energy transfer processes and depends on the distribution functions of donors and acceptors, which in turn are linked to the concentration profiles of the polymer at the interface. The detailed analysis of FRET in such systems required the development of energy transfer models that correctly consider the topological constraints of the medium and the donor and acceptor distributions arising from polymer diffusion.[19,20]

Most previous experiments on interparticle polymer diffusion during latex film formation were carried out on linear polymers, with the intent of understanding how the properties of the latex polymer evolve.[19−23] Recently, we began to examine diffusion in branched or partially cross-linked polymers, such as poly(vinyl acetate), PVAc. Homopolymers of VAc and its copolymers are normally extensively branched.[24] This intrinsic branching occurs during the polymerization reaction, caused by chain transfer of the highly reactive PVAc radical in one polymer chain to a methyl side group (by hydrogen abstraction) of another chain. In copolymers of PVAc, the comonomer is often the source of reactive hydrogen atoms along the polymer backbone, usually causing the copolymers to be more branched than the PVAc homopolymer. Although branching itself does not lead to gel formation, these systems are often characterized by a significant gel content as a consequence of termination reactions between growing chains. The gel domains themselves have diameters that are limited by the size of the latex particles. Within films formed from these particles the cross-linked domains are present as "nanogels" confined to individual polyhedral cells. We imagine that they undergo very little or very slow diffusion in these latex films. In addition, some chains in the system may contain entangled long-chain branches which can severely suppress chain mobility.[5] These chains are likely to remain diffusively immobile on a time scale during which the shorter and less branched polymers can diffuse across the interface between particles.

Recently FRET measurements were used to study polymer diffusion in films of copolymers of vinyl acetate (VAc) and dibutyl maleate (DBM).[25,26] One sample, prepared without chain transfer agent, had a measured gel content of 50 wt %. We were able to separate and analyze the sol and gel components of this sample. A second sample, prepared with a chain transfer agent, had no detectable gel content and a nominal molecular weight of ca. 250000. The polymers were labeled either with 9-methacryloxymethylphenanthrene (PheMMA, structure **I**) as a donor dye or with 2′-acryloxy-4′-methyl-4-(*N*,*N*-dimethylamino) benzophenone (NBen, structure **II**) as acceptor.

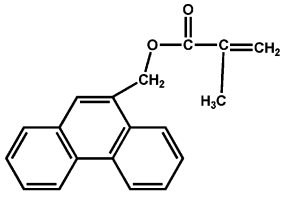

PheMMA

Structure **I**

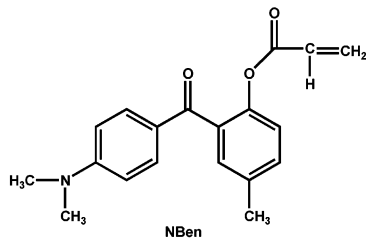

NBen

Structure **II**

It turned out that the sol fraction of the first sample had a GPC trace similar to that of the second sample, indicating that both components had a similar molecular weight distribution. The polymers in latex films formed from the two samples, underwent interparticle polymer diffusion at similar rates, but in the gel-containing sample only a fraction of the polymer present in the sample was able to diffuse across these boundaries, whereas, in the gel-free sample, most of the polymer was able to undergo diffusive mixing with the polymer molecules in neighboring cells. It was concluded that only the sol component of the gel-containing polymer was able to diffuse on the time scale of the experiments, and the diffusion rate of the mobile component and its temperature dependence in the gel-containing polymer were comparable to that of the gel free counterpart.[27]

In this paper, we return to these results and attempt to model the diffusion of the mobile chains in the presence of gel nanodomains, each occupying one latex

particle. The challenge is to develop a meaningful model of polymer diffusion in this system, and then connect the diffusion of polymers segments across the interparticle boundaries to the growth in energy transfer in the system. We based our approach on the previously reported model for FRET between dyes attached to linear polymer chains diffusing across the interface between cells in latex films.[19,23] Here, we examine the diffusion of the mobile component and take into consideration the presence of gel nanodomains in the film that contain covalently bound donor or acceptor dyes, but are immobile during the diffusion process.

We analyze the FRET data by two methods. In our traditional simplified approach,[21] we fit experimental donor decays to a stretched exponential function. From the areas under each fitted donor decay profile, we calculate the quantum efficiency Φ_{ET} of energy transfer. We use these values to calculate an operational "extent of mixing" parameter f_m (see below). This parameter corrects for the small amount of energy transfer across the interparticle boundaries in the newly formed films and monitors the fractional growth in Φ_{ET} due to polymer diffusion. To estimate the extent of diffusion of the mobile polymer chains in the latex films, we assume that f_m is in fact equal to the fractional mass f_s that has diffused across the initial particle boundaries. This is a crude approach, but it allows us to calculate an apparent diffusion coefficient D_{app} that, for linear polymers, approximately follows the "true" average diffusion coefficient.[19,23]

We next analyzed the same experimental data using a more fundamental model that we developed to account for the effect of the gel nanodomains. This new model describes the shape of the donor fluorescence decay profile taking into account the detailed mechanism of energy transfer from the donor to the acceptor dyes and the diffusion of the soluble polymer in the presence of the gel nanodomains in the polymer film. We fit our experimental donor fluorescence decays using donor fluorescence survival probability curves simulated with this model. From the polymer segment density profile thus obtained, we determine an average diffusion coefficient $\langle D \rangle$ for the polymer as a function of annealing time.

Experimental Part

The Latex Samples. The synthesis and characterization of PheMMA- and NBen-labeled gel-containing poly(VAc-DBM) latex samples have been described elsewhere.[25] The polymer was prepared via a conventional batch emulsion polymerization process from 4:1 wt ratio (10.6:1 mol ratio) of VAc:DBM with an uniform composition throughout the polymerization. The latex polymer has a gel content of ca. 50% and the sol fraction has $M_w = 280000$ and $M_n = 107000$, $M_w/M_n = 2.6$ (GPC, using polystyrene standards). The labeled poly(VAc-DBM) polymers have uniform dye distribution along the polymer chains—a characteristic very important for the FRET study. This pair of latex particles has similar particle size (124 nm) and narrow size distribution. A corresponding unlabeled poly(VAc-DBM) copolymer has a major glass transition at ca. 24 °C and a minor glass transition at ca. 34 °C.

Fluorescence Measurements. For fluorescence decay measurements, latex films (prepared as described in ref 25) were placed in a quartz tube, sealed and degassed by flowing nitrogen for 3−5 min before and after each measurement. Fluorescence decay profiles were measured by the time-correlated single photon timing technique.[28] The excitation wavelength was 300 nm, and emission from the sample was detected through a combination of a band-pass filter (310−400 nm) and a cutoff filter (335 nm) to minimize the amount of scattered excitation light reaching the detector. In the absence of NBen, samples containing 1 mol % donor PheMMA show decay profiles that can be fitted with only one exponential function, with a lifetime $\tau_D = 44.6$ ns.

Data Analysis

The quantum efficiency of energy transfer $\Phi_{ET}(t)$ is defined as

$$\Phi_{ET}(t_{diff}) = 1 - \frac{\int_0^\infty I_{DA}(t)\,dt}{\int_0^\infty I_D(t)\,dt} \tag{1}$$

where the integral of $I_D(t)$ is the area under the donor decay profile of a film containing only donor. Since the unquenched donor decay profiles for the phenanthrene derivatives employed here are exponential, the value of the integral equals the unquenched donor lifetime τ_D. The integral of $I_{DA}(t)$ describes the area under the donor decay profile of a film containing both donor and acceptor, annealed for a time t_{diff}. The quantum efficiency of energy transfer can then be evaluated as

$$\Phi_{ET}(t_{diff}) = 1 - \frac{\text{area}(t_{diff})}{\tau_D} \tag{2}$$

In our simplified traditional approach, we obtain the area for each decay profile by fitting the decay curves to the empirical eq 3 and then evaluate the integral analytically from the magnitude of the fitting parameters.

$$I_D(t) = A_1 \exp[-t/\tau_D - P(t/\tau_D)^{1/2}] + A_2 \exp(-t/\tau_D) \tag{3}$$

We then approximate the extent of mixing f_m that occurs upon annealing a film for a time t_{diff} by the corresponding fractional increase in the quantum efficiency of energy transfer

$$f_m(t_{diff}) \approx \frac{\Phi_{ET}(t_{diff}) - \Phi_{ET}(0)}{\Phi_{ET}(\infty) - \Phi_{ET}(0)} = \frac{\text{area}(0) - \text{area}(t_{diff})}{\text{area}(0) - \text{area}(\infty)} \tag{4}$$

where $[\Phi_{ET}(t_{diff}) - \Phi_{ET}(0)]$ represents the change in ET efficiency between the initially prepared film and that annealed for a time t_{diff}. The term $[\Phi_{ET}(\infty) - \Phi_{ET}(0)]$ represents the maximum change in FRET efficiency, between the initially prepared film and the fully mixed film. Within this approximation, the extent of mixing parameter f_m can be directly calculated by comparing the areas under the decay profiles for films annealed for various times, area(t_{diff}), to that of a film without annealing, area(0), and to one cast from a solution to approach the value for full mixing, area(∞). Conceptually this is a drastic approximation, but simulations for one-dimensional diffusion in latex films that satisfy Fick's law show that f_m is proportional to the real fraction of diffusing substance (mass fraction of mixing, f_s), for values of f_m up to ca. 0.7.[29] Therefore, f_m is a convenient parameter to characterize the extent of polymer diffusion in latex films, since it is simple to obtain and it approximately follows the evolution of the mass fraction of mixing with annealing time.

The diffusion coefficient is a fundamental parameter to characterize the rate of polymer diffusion across the

latex particle interface. It can be calculated at different levels of rigor and sophistication.[29−33] In our traditional approach, apparent diffusion coefficients D_{app} were calculated from f_m, assuming that $f_m = f_s$, where f_s is the real fraction of the mass that has diffused across the initial boundary, and fitting the data to a spherical Fickian diffusion model.[34] The strengths and weaknesses of this analysis have been discussed previously for latex films consisting of linear polymer.[19,23,29] The apparent mean diffusion coefficient D_{app} represent an average over the broad polymer molecular weight distribution of the sample and an integration over the sample history. Therefore, values of D_{app} from different samples can be compared only at similar values of f_m. The importance of these numbers is that, for samples with similar degrees of acceptor labeling, changes in D_{app}, compared at similar f_m values, closely follow changes in the true center-of-mass diffusion coefficients of the polymers.[29]

In our gel-containing sample, the maximum apparent extent of mixing is only 40% (as calculated from f_m). This leads to a concern about the validity of the traditional simplified approach to calculate the diffusion coefficient (D_{app}) and consequently the feasibility of using these D_{app} values to calculate an Arrhenius activation energy (E_a) for polymer diffusion. For the sample in question, this approach does yield the same temperature dependence of diffusion as obtained from rheology measurements (dynamic moduli G', G'' vs frequency at a series of fixed temperatures.[26] Nevertheless, to understand the nanometer-scale dynamics of the present system, we have developed a more sophisticated and hopefully more general model to simulate the dye-labeled polymer concentration profiles in the presence of gels, and to obtain the corresponding fluorescence donor decay profiles that can later be compared to experimental curves.

In our new approach, we assume that the gel nanodomains occupying each cell do not move during the experiment, and calculate the donor and acceptor concentration profiles generated by the diffusion of the soluble polymer fraction across the particle interfaces. These concentration profiles can be directly used to generate donor survival probabilities using the theory of energy transfer in restricted geometry.[19,29,35] For a δ-pulse excitation, the excited donor survival probability $I^s_D(t)$ depends on the distribution of both acceptors and donors[19]

$$I_D{}^s(t) = \exp\left(-\frac{t}{\tau_D}\right)\int_{V_s} C_D(r_D)\varphi(t,r_D)r_D{}^2 \mathrm{d}r_D \quad (5a)$$

$$\varphi(t,r_D) = \exp\left(-\frac{2\pi}{r_D}\int_{R_e}^{\infty}\{1 - \exp[-w(r)t]\}\left[\int_{|r_D-r|}^{r_D+r} C_A(r_A)r_A \mathrm{d}r_A\right]r\mathrm{d}r\right) \quad (5b)$$

In these equations V_s is the volume containing the donors that were initially confined to a donor-labeled particle, $\varphi(t, r_D)$ is the energy transfer probability from a donor at r_D to any of the acceptors around, $C_D(r)$ and $C_A(r)$ are the concentration profiles of donors and acceptors, and the encounter radius R_e, is the minimum distance between donor and acceptor (this is usually considered to be equal to the sum of the donor and acceptor van der Waals radii).[36] The rate of energy transfer between one donor and one acceptor for a dipole−dipole coupling mechanism at the separation distance r is given by[37]

$$w(r) = \frac{\alpha}{r^6}; \quad \alpha = \frac{3R_0{}^6\kappa^2}{2\tau_D} \quad (6)$$

Here, τ_D is the unquenched donor lifetime, κ^2 is a dimensionless parameter related to the relative orientation of the donor and acceptor transition dipole moments (for a random distribution of dipoles, immobile on the time scale of the donor lifetime $\langle\kappa\rangle^2 = 0.476$),[38] and R_0 is the characteristic (Förster) distance defined as[39]

$$R_0{}^6 = \frac{9000(\ln 10)\kappa^2 Q_D}{128\pi^5 N n^4}\int_0^{\infty} F_D(\lambda)\epsilon_A(\lambda)\lambda^4 \mathrm{d}\lambda \quad (7)$$

where Q_D is the quantum yield of the donor in the absence of acceptor, N is Avogadro's number, n is the refractive index of the medium, $F_D(\lambda)$ is the fluorescence intensity of the donor at wavelength λ (with the total intensity normalized to unity), and $\epsilon_A(\lambda)$ is the extinction coefficient of the acceptor at the wavelength λ.

To analyze experimental data through simulations, one convolutes the trial decay function $I_D{}^s(t)$ calculated from eq 5 using test donor and acceptor concentration profiles with the experimental lamp profile, and compares the resulting simulated donor decay curve with the experimental curve. We used a coarse grid mapping of the parameter space to locate the main minima and identify the desired parameter range over which the search should be refined. For each set of input parameters in the simulation we calculated the reduced χ^2.[40,41] The best fitting of an experimental decay is characterized by random distribution of both the weighted residuals and the autocorrelation of weighted residuals.

Results and Discussion

Poly(VAc-*co*-DBM) latex films containing only Phe exhibit a single-exponential fluorescence decay curve with a lifetime $\tau_D = 44.6$ ns. On the other hand, latex films prepared from a mixture of Phe- and NBen-labeled poly(VAc-*co*-DBM) latex dispersions exhibit nonexponential donor fluorescence decay profiles due to energy transfer from the donor to the acceptor dyes. In freshly prepared films (cast just above the MFT) the efficiency of energy transfer is low and is related to energy transfer occurring across the interface. After annealing at higher temperatures, polymer diffusion across the intercellular boundaries in the film leads to mixing of donor- and acceptor-labeled polymer, with a strong increase in Φ_{ET}. When the donor fluorescence decay curves are fitted with eq 3 and the quantum efficiency of energy transfer $\Phi_{ET}(t_{\mathrm{diff}})$ is calculated from eq 2 for different annealing temperatures t_{diff}, we observe that there is a large increase in Φ_{ET} at early times, followed by a smaller increase at longer times (Figure 1). For all the tested annealing temperatures, the limiting value of Φ_{ET} is much lower than the value of Φ_{ET} for films obtained by solvent-casting from a 1:1 mixture of the soluble fractions of donor- and acceptor-labeled polymer, $\Phi_{ET}(\infty) = 0.52$.[26] This is a consequence of the gel content of the latex sample, which limits the extent of diffusive mixing of the non-cross-linked polymers.

Apparent Diffusion Coefficients. Using our simple approach, we evaluate the extent of diffusion in the latex

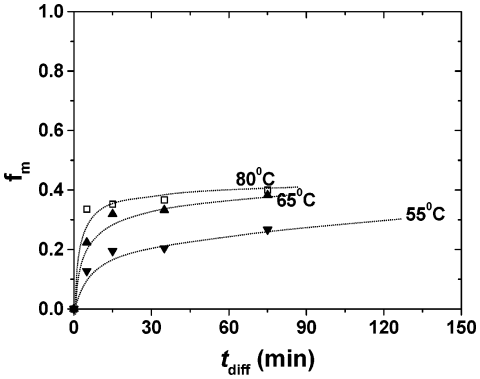

Figure 1. Fractional increase in the quantum efficiency of energy transfer vs annealing time for poly(VAc-*co*-DBM) latex films annealed at 55, 65, and 80 °C.

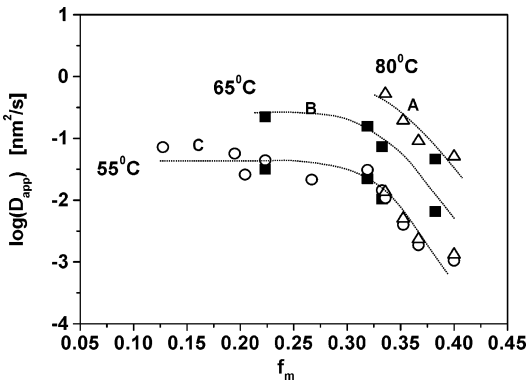

Figure 2. Values of the apparent diffusion coefficient D_{app} plotted against the apparent extent of mixing f_m. The data obtained at 80 and 65 °C are also shown after being recalculated to 55 °C using $E_a = 37$ kcal/mol.

films at the level of the evolution of the energy transfer quantum efficiency. We approximate the extent of mixing that occurs upon annealing a sample for a time t_{diff} by the parameter f_m characterizing the fractional evolution of the quantum efficiency of energy transfer, calculated using eq 4 and with $\Phi_{ET}(\infty) = 0.52$, corresponding to a fully randomized distribution of donors and acceptors in these films. We consider that f_m is equal to the true mass fraction of mixing f_s and evaluate the mean apparent diffusion coefficient D_{app}, using the equation for Fickian diffusion in spherical symmetry.[34] In this simple model, we did not consider the effect of gel directly, but we normalized our apparent mixing, taking into consideration the full amount of mixing that we would obtain in the absence of gel. While both f_m and the real extent of diffusion increase from 0 to reach a maximum of 1 (for full mixing in the absence of gel), they measure different consequences of polymer diffusion. In Figure 2 we plot D_{app} values calculated in this way against f_m. The tendency for a strong decrease of D_{app} with increasing f_m is attributed to the broad polydispersity of the polymer chains in latex samples obtained by emulsion polymerization. We also notice that these values increase markedly with the annealing temperature. An Arrhenius plot of $\mathrm{Ln}(D_{app})$, at constant f_m, gave an apparent activation energy of ca. 37 kcal/mol.[26]

Rate of Polymer Interdiffusion. We have seen before that the apparent degree of polymer mixing f_m is a fair approximation of the real fraction of mixing in latex films for un-cross-linked latex samples.[19,23,29] However, f_m alone is not precise enough to quantify the rate of polymer diffusion in an absolute way. The ideal parameter to characterize the polymer diffusion rate would be the distribution of center-of-mass diffusion coefficients. This is a daunting task. A more accessible quantity, for a polydisperse system, is the mean diffusion coefficient $\langle D \rangle$, which characterizes the rate at which a certain fraction of the mass has diffused across the intercellular boundary. Since the system is in reality characterized by a distribution of species with different diffusivities, the magnitude of $\langle D \rangle$ will decrease with time as the less mobile species diffuse across the interface. In the past, we have taken several approaches to simulate FRET experiments on latex films in terms of an evolving mean polymer diffusion coefficient.[19,23,29,42,43] In our previous work, we have assumed that the general shape of the polymer segment distribution can be described by Fickian diffusion for spherical geometry.[34] This yields the following distributions of the donor and acceptor dyes (g_D and g_A) in neighboring particles [19,29]

$$g_D(r') = \frac{1}{2}\left(\mathrm{erf}\left(\frac{1+r'}{\theta}\right) + \mathrm{erf}\left(\frac{1-r'}{\theta}\right) + \frac{\theta}{\sqrt{\pi}r'}\left\{\exp\left[-\left(\frac{1+r'}{\theta}\right)^2\right] - \exp\left[-\left(\frac{1-r'}{\theta}\right)^2\right]\right\}\right) \quad (8a)$$

$$g_A(r') = g_D(2 - r') \quad (8b)$$

where $\theta = 2\,(\langle D \rangle\, t_{diff})^{1/2}/R_s$ is a parameter measuring the extent of diffusion, t_{diff} is the diffusion time, $\langle D \rangle$ is the mean diffusion coefficient, R_s is the radius of the particle, and $r' = r/R_s$ measures the fractional distance from the center of a particle. From the distribution profiles we can calculate the volume fraction of polymer mixing f_s using

$$f_s = 1 - 3\int_0^1 4\pi r^2 g_D(r')\mathrm{d}r' \quad (9)$$

The presence of gel, detected experimentally, requires a more complex model to describe the distribution profiles. We have to take into account the effect on the energy transfer signal of the gel nanodomains and of the concentration profile generated by the diffusion of the un-cross-linked chains through the particle boundary. We start by assuming that the gel nanodomains in poly(VAc-*co*-DBM) latex films do not move upon annealing. This assumption is supported by the experimental results in which we compared the diffusion in gel-containing and gel-free poly(VAc-*co*-DBM) latex films: we found that the sol fraction of the gel-containing polymer makes the major contribution to the diffusion in the gel-containing latex film.[25] More important, in neutron reflectometry studies of the interface between polystyrene networks as reported by Geoghegan et al.,[44] it is apparent that the interface width between polystyrene networks does not change as a function of annealing time or temperature.

Another aspect of our samples is that the number-average molecular weight of the polymer soluble fraction is about nine times higher than the entanglement molecular weight of PVAc ($M_e = 12000$).[45] Therefore, even those chains that are not cross-linked or appreciably branched, will present entanglements. The chains will then diffuse by a mechanism that combines reptation with segmental motion.[5] For times shorter than the reptation time, τ_r, reptation dominates the

chain motion. At longer times, successive displacements of the chain are statistically independent, and over large time scales the dynamics of the polymer can be described by the Fickian motion of its center-of-mass. In conclusion, the diffusion of polymer chains across an interface is very complex for $t < \tau_r$,[7,8] but for times longer than τ_r, we can describe the chain dynamics by the diffusion of its center-of-mass with the corresponding concentration profiles given by the solution of Fick's equations.

It is therefore important to have an idea of the mean reptation time for our sample. For linear chains, this value can be estimated from $\tau_r = R^2/(3\ \pi\ D)$,[6] where R is the end-to-end distance of the polymer and D is the corresponding diffusion coefficient. Following the approximations used by Wool[8] to calculate the reptation time relative to results obtained by Winnik,[46] we first estimate $R \approx 30$ nm for the molecular weight corresponding to the weight-average molecular weight of the soluble polymer fraction in our samples, $M_w = 280000$. For this fraction, and using a diffusion coefficient value corresponding to an intermediate cumulative diffusion time from our data in Figure 2 ($D \approx 0.05$ nm^2 s^{-1}), we obtain $\tau_r = 10$ min. This means that for most diffusion times accessible to our experiments, linear polymer chains with molecular weight $M = 280000$ will probably be well described by a Fickian diffusion profile.

However, our PVAc samples consist mainly of branched polymer chains. The effects of branching on the polymer diffusion mechanism and on the reptation time are not yet well described experimentally. Theoretically, the reptation time increases exponentially with the length of the branches, with diffusion being severely decreased or even completely suppressed in polymers with long polymer branches.[5] Therefore, diffusion coefficients are much smaller in a branched polymer than in its linear counterpart of the same molecular weight.[5] In our sample, we expect that the number and molecular weight of the branches increases with chain molecular weight so that, in smaller chains the effect of branching in diffusion will be minimal, while the larger chains will be practically immobile. In our approach, we will consider that the smaller chains will have reptation times short enough for their diffusion to be described by a Fickian profile for all accessible diffusion times. On the other hand, the highly branched larger chains, having arms that are long enough for reptation to impair diffusion through the film, will be considered as part of the immobile gel fraction of the polymer. This is a reasonable approximation in view of earlier results by Antonietti and Sillesco,[47] regarding the diffusion of linear polystyrene (PS) chains with molecular weights from M_e to $5M_e$ into model PS networks. They showed that the diffusion coefficients of the linear chains where approximately the same for the diffusion into cross-linked networks or into matrices of linear entangled chains of $M_w = 6\ M_e$.

The concentration profile of the polymer initially contained in a particle is therefore described as a function of the amount of gel and the extent of mixing between the polymer chains from neighboring particles. As discussed above, we will assume that the general shape of the polymer segment distribution can be described by the superposition of an immobile gel phase distribution and a Fickian [34] diffusion profile. The distributions of the donor and acceptor dyes (g_D and g_A) from two neighboring particles are then given by

$$g_D(r') = f_{gel}\mathrm{H}(1-r') + 0.5(1-f_{gel}) \times \left(\mathrm{erf}\left(\frac{1+r'}{\theta}\right) + \mathrm{erf}\left(\frac{1-r'}{\theta}\right) + \frac{\theta}{\sqrt{\pi}r'}\left\{\exp\left[-\left(\frac{1+r'}{\theta}\right)^2\right] - \exp\left[-\left(\frac{1-r'}{\theta}\right)^2\right]\right\}\right) \quad (10a)$$

$$g_A(r') = g_D(2-r') \quad (10b)$$

where θ and r' have the same meaning as in eqs 8. The function H is the unit step function, and f_{gel} is the gel fraction of the sample. In Figure 3 (top), we show the distribution functions for film with gel content of 50% and increasing diffusion times (increasing θ values). From the distribution profiles we can calculate the volume fraction of polymer mixing (f_s) using eq 9. This parameter increases almost linearly with θ within the range of values shown (Figure 3, bottom).

The $\langle D\rangle$ values recovered from θ, $\langle D\rangle = (\theta\ R_s/2)^2/t_{diff}$, describe the mean cumulative diffusion coefficient. The evolution of these values with diffusion time reflects the complex composition of the system. The species with lower molecular weight are less branched and more mobile, making the major contribution to the early mean cumulative diffusion coefficient. On the other hand, higher molecular weight species will move slower, making a larger contribution to the mean cumulative diffusion coefficient at longer diffusion times. As previously discussed, there is probably a fraction of high molecular weight chains with long-chain branches that are practically immobile for the experimentally accessible diffusion times.

Mean Cumulative Diffusion Coefficients. When we describe our gel-containing poly(VAc-*co*-DBM) system using eq 10, the final concentration profile is a combination of the gel and sol fraction contributions. Since we assume that gel domains do not diffuse during the experiments, the number of variables in the new model is not increased compared to eq 8 because the gel fraction was measured experimentally. We next relate the shape of the concentration profile of the polymer initially contained in a particle, to the donor fluorescence decay profile for energy transfer between dyes attached to polymer chains in neighboring latex particles forming a solid film. The donor and acceptor dyes are assumed to be attached at random to the polymer chains, so that the spatial distribution of dyes follows the segment distribution of the individual polymer chains. The dyes attached to polymer in the gel phase cannot leave the initial particle boundaries. As the other polymer chains (forming the sol phase) diffuse across the interface between particles, donor and acceptor dyes come into close proximity and the energy transfer efficiency increases (Figure 4). This increase is used to determine the concentration profile of the polymer.

Since the donor and acceptor dyes are randomly attached to the polymer chains, the concentration profiles of donors and acceptors that appear in eq 5, $C_D(r)$ and $C_A(r)$, are related to the polymer concentration profiles of eq 10: we consider $C_D(r) = g_D(r)$ and $C_A(r) = C^0_A\ g_A(r)$, with C^0_A being the initial average number density of acceptors in the acceptor labeled particles.

To evaluate eq 5 using the distribution functions of eq 10, we calculate all the integrals using a simple trapezoidal rule because adaptive quadrature routines are not stable in the evaluation of multiple integrals.[48]

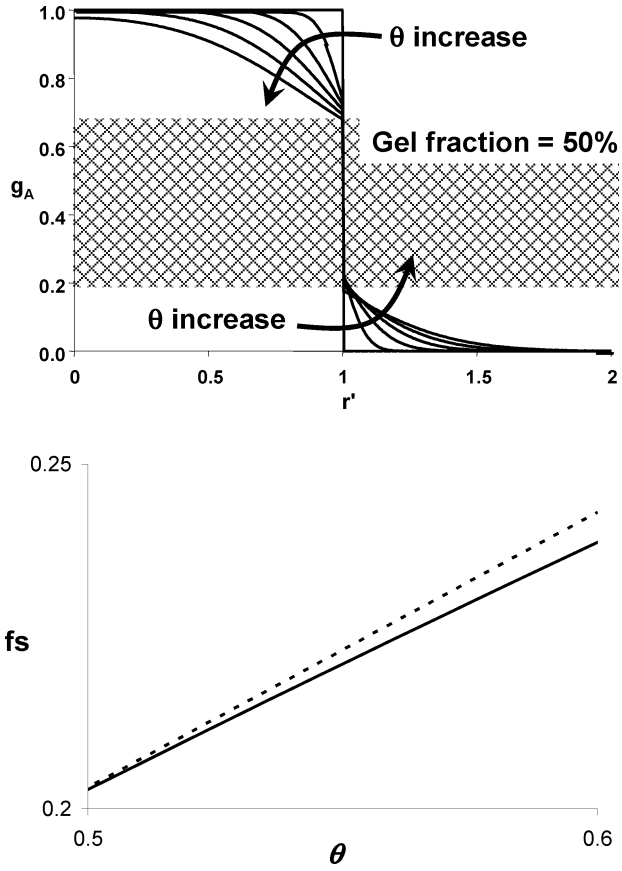

Figure 3. Polymer density distribution functions (top) in a spherical cell of radius R_s with gel content of 50%, calculated according to eq 11 for $\theta = 0$, 0.1, 0.2, 0.3, 0.4, 0.5, and 0.6. The volume fraction of mixture f_s (bottom, dotted line) increases almost linearly with θ (the solid line represents a linear relation.

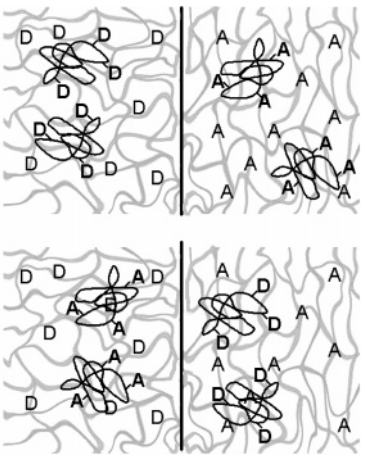

Figure 4. Donor and acceptor dyes are randomly attached to the polymer chains in the gel and the mobile components (top). The dyes attached to the polymer composing the gel phase cannot leave the initial particle boundaries. As the mobile polymer chains diffuse across the interface between cells in the latex film (bottom), donor and acceptor dyes come into close proximity and the extent of energy transfer is increased.

Also, since $w(r)$ is a very sharply peaked function of r for all accessible experimental times, the integration over r was evaluated only from R_e to $3R_0$.

We start by simulating a series of donor fluorescence decay functions calculated using eqs 5 and 10, for $\theta =$ 0 to 0.6, using $\kappa^2 = 0.476$, $R_0 = 2.51$ nm, $\tau_D = 44.6$ ns

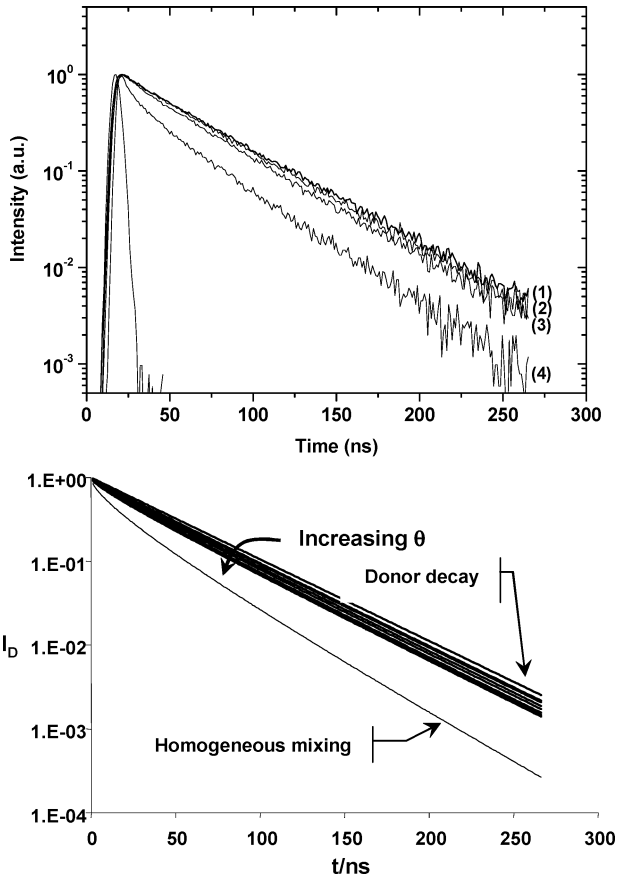

Figure 5. Donor fluorescence decay profiles (top) of a poly(VAc-*co*-DBM) film labeled with donor only (1), a nascent film formed at room temperature, prepared from a 1:1 ratio of PheMMA-labeled poly(VAc-*co*-DBM) and NBen-labeled poly(VAc-*co*-DBM) latex particles (2), a similar film annealed at 100°C for 2 h (3), and a film formed from the isolated sol fraction of the poly(VAc-DBM) and then cast from 1,4-dioxane solution (4). This film consists of a 1:1 ratio of donor-labeled- and acceptor-labeled polymer. Simulated donor survival probability curves (bottom) for $\theta = 0$ to 0.6, calculated using eqs 5, 11 with $\kappa^2 = 0.476$, $R_0 = 2.51$ nm, $\tau_D = 44.6$ ns, $R_e = 0.5$ nm and an initial average concentration of acceptor $C_{A0} = 0.03$ M.

and a cutoff distance $R_e = 0.5$ nm (parameters for the Phe-NBen donor−acceptor pair). From independent experimental data we know that the donor-labeled particle has a radius $R_s = 62$ nm (dynamic light scattering),[49] a gel content $f_{gel} = 0.5$ (solvent extraction), and an average acceptor concentration in the film $C^0_A = 0.03$ M. In Figure 5, we show both the experimental donor decay profiles (Figure 5, top), and the simulated donor survival probability curves for $\theta = 0$ to 0.6 (Figure 5, bottom), which correspond to the donor distribution profiles shown in Figure 3. We note that, as the amount of mixing increases, more donors and acceptors come into proximity, energy transfer efficiency increases, and the donor decays faster. We also point out that for $\theta =$ 0 nm the donor fluorescence survival probability represents the amount of energy transfer taking place across a perfectly sharp spherical interface. The maximum amount of mixing in both cases is much lower than the complete mixing obtained in a film prepared by solvent casting the sol fraction of donor and acceptor labeled poly(VAc-*co*-DBM).

To analyze experimental data using the curves simulated with the new model, we convolute the simulated trial decay function $I^s_D(t)$ with an experimental instru-

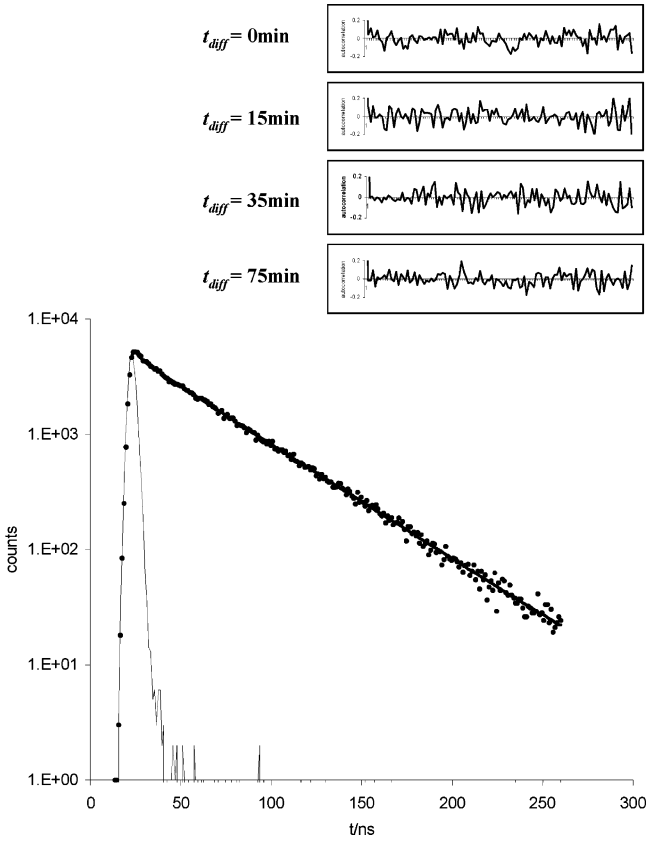

Figure 6. Experimental instrument response function and experimental donor decay profile measured for a film of poly(VAc-*co*-DBM) (bottom), dried at room temperature and fitted to a decay simulated with $\theta = 0.07$. The solid line represents the fitted decay and the dotted line the experimental decay; Autocorrelation function plots (top) for the fitting of the experimental curves of the dried film ($t_{diff} = 0$) and films annealed for 15, 35, and 75 min at 80 °C, to curves simulated with $\theta = 0.27$, 0.30, and 0.34.

ment response function (or lamp profile), $L(t)$, obtained from the experimental excitation source [50]

$$I_D^{conv}(t) = \int_0^t L(s) I_D(t - s)\, ds \qquad (11)$$

Then we compare the resulting simulated fluorescence decay curve with the experimental decay curves using a linear fitting algorithm where the fitting parameters are the normalization factor of the decay intensity a_N, and the light scattering correction a_L [51]

$$I_D^{exp}(t) = a_L L(t) + a_N I_D^{conv}(R_s,t) \qquad (12)$$

Modifying the input parameters of the simulation, we can obtain the best fit as determined by minimization of the χ^2 parameter. Good fits are characterized by a random distribution of both the weighted residuals and the autocorrelation of weighted residuals.

In Figure 6, we show the experimental donor decay profile measured for a film of poly(VAc-*co*-DBM) freshly dried at room temperature (bottom) and its best fitting to the theoretical model, which is obtained for a decay simulated with $\theta = 0.07$. The autocorrelation function plots (top) for the best fittings of the experimental curves of films, immediately after drying ($t_{diff} = 0$) and subsequently annealed for 15, 35, and 75 min at 80 °C, indicate good agreement between the new model and the experimental decays. The best fitting results for

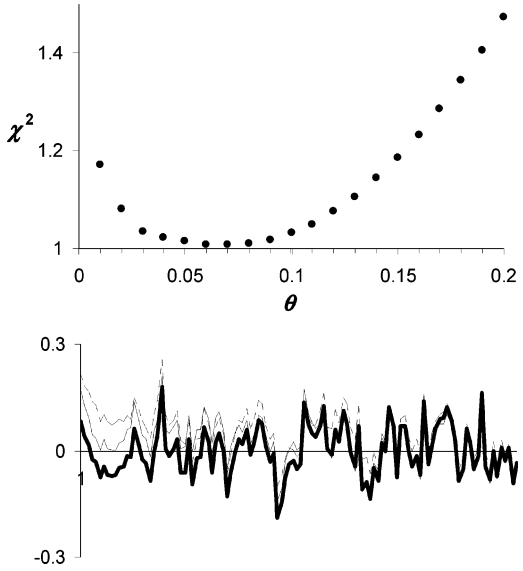

Figure 7. Variation in the reduced χ^2 parameter (top) in the analysis of an experimental donor decay profile measured for a film of poly(VAc-*co*-DBM) freshly dried at room temperature ($t_{diff} = 0$) using curves simulated with different values of θ. The autocorrelation of weighted residuals (bottom) obtained for the fitting with a curve simulated for 0.07 (dark line) shows a better distribution than for $\theta = 0.05$ (thin line) and 0.09 (broken line).

decays measured at $t_{diff} = 0$, 15, 35, and 75 min are obtained for curves simulated with $\theta = 0.07$, 0.27, 0.30, and 0.34. Here, we fit the experimental donor decay profiles starting before the maximum of the excitation profile and obtain well-distributed autocorrelation plots of the weighted residuals. The parameters a_N and a_L (the decay-intensity-normalization and the light-scattering-correction respectively) obtained for the best fitting of the experimental data, do not change significantly with annealing temperature or diffusion time.

To establish the accuracy in the values of θ recovered from our analysis, in Figure 7 (top) we show the variation in the reduced χ^2 parameter with θ for the analysis of an experimental donor decay profile measured for a film of poly(VAc-*co*-DBM) freshly dried at room temperature ($t_{diff} = 0$). This gives us an indication that the accuracy in the determination of θ is of the order of 0.02, with the best result corresponding to $\theta = 0.07$. This is further confirmed by comparing the plots of the autocorrelation of weighted residuals (Figure 7, bottom) obtained for the fitting of the same experimental decay to curves simulated with $\theta = 0.05$, 0.07, and 0.09. We can then conclude that the uncertainty in the determination of $\langle D \rangle$ is lower than 10−15% for typical values of θ around 0.3.

In Figure 8 (top), we show the volume fraction of mixing f_s calculated from the best-fit θ values obtained for poly(VAc-*co*-DBM) films annealed at 55, 65, and 80 °C. As expected, the amount of mixing increases faster for higher annealing temperatures due to faster diffusion.

For the films dried at room temperature, we calculate that there is about 3% of mixing between donor and acceptor labeled chains before any annealing. This initial mixing is much lower than that found for uncross-linked PBMA samples,where about 8% of initial mixing was found using a similar method of analysis.[23] The value obtained in the present work is related to the very small amount of mixing between particles that

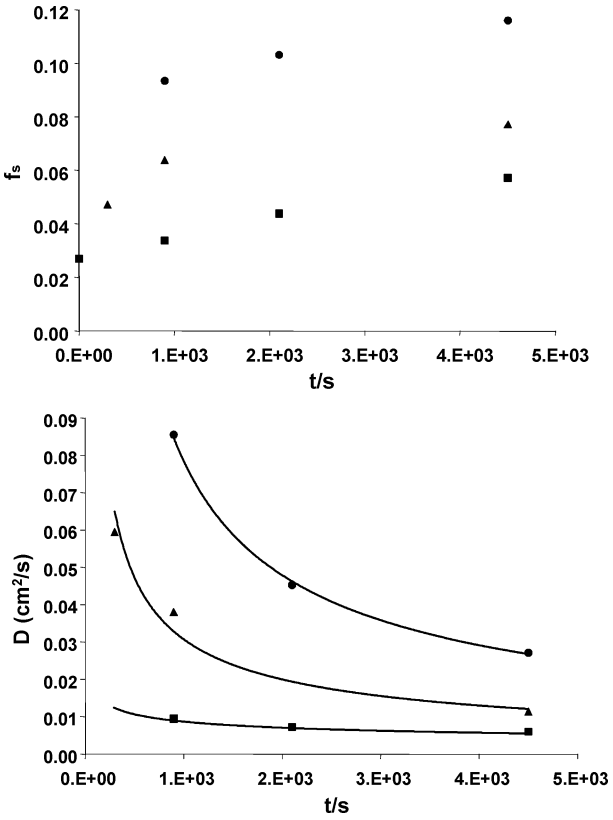

Figure 8. Volume fraction of mixing (top) obtained for films annealed at 55 (■), 65 (▲), and 80 °C (●), and diffusion coefficients corresponding to the fitted θ values (bottom).

takes place during film drying, caused by the polymer chain ends close to the interface or the diffusion of low molecular weight component of the latex. This effect is neatly explained in terms of the roughness of the particle surface, which leads to a waviness of the interface between adjacent cells in the film.[52] Indeed, neutron reflectometry measurements of the interface between polystyrene (PS) networks conducted by Geoghegan showed that the interface between two networks could be described by a Gaussian roughness profile.[44] Possible origins of this roughness are as follows: (i) chain interpenetration across the interface due to the swelling effect of solvent trapped in the network; (ii) dangling chain ends in the network that can stretch across the interface; (iii) network heterogeneities with regions of lower cross-linking density; (iv) an entropic effect that leads the contacting networks to stretch and contract in order to substitute an undesirable sharp contact surface by a bumpy interface.[44]

The average diffusion coefficient $\langle D\rangle = (\theta R_s/2)^2/t_{\text{diff}}$ calculated from the best-fit θ values, decrease with increasing annealing time (Figure 8, bottom) reflecting the contribution of higher molar mass polymers (with lower diffusivities) to the growth in FRET for longer annealing times.

The initially high average diffusion coefficient can also have a contribution from the initial rapid partial interdigitation of the free chain ends of highly branched and cross-linked chains that are anchored to the gel network of one particle into a neighboring particle. These can only stretch for a limited distance into the gel network of a neighbor particle and so would only contribute to the growth in energy transfer at shorter annealing times. This effect was described by Geoghegan for the penetration of grafted PS chains into PS networks.[53] In these experiments there is an initial rapid partial interdigitation of the grafted chains into the network, followed by a very slow relaxation to form the equilibrium interface.

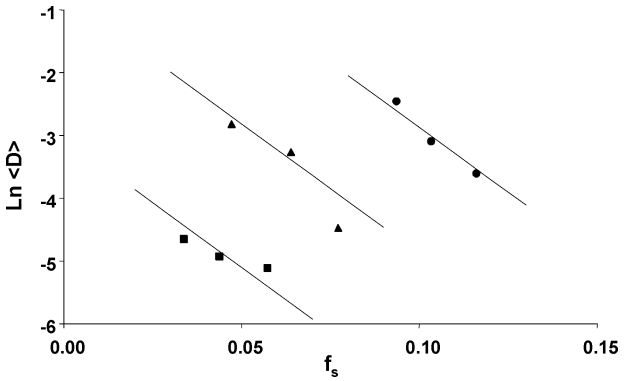

Figure 9. Multilinear fit of the data points in Figure 7, for 55 (■), 65 (▲), and 80 °C (●), yields a diffusion activation energy of 39 kcal/mol.

In Figure 8 (bottom), we also note that the $\langle D\rangle$ values increase with increasing temperature. If we plot the diffusion coefficients $\langle D\rangle$ as a function of the extent of mixing f_s, we can access the effect of temperature on diffusion at comparable extents of mixing (Figure 9). Fitting these data to three parallel lines (in a multilinear fitting procedure) and analyzing the result in an Arrhenius fashion, we obtain an effective activation energy for diffusion of 39 ± 5 kcal/mol. This result is in good agreements with rheological measurements on the same sample, performed at different temperatures to follow the response of the dynamic moduli (G', G'') with respect to the frequency.[26]

Conclusions

We reexamined experiments reported by Wu et al. which employed Förster resonance energy transfer (FRET) measurements to follow polymer interdiffusion in films cast from gel containing, dye labeled, poly(VAc-*co*-DBM) latex dispersions. The data were analyzed in two distinct ways. Using a simplified approach, we calculated f_m values from the quantum efficiency of energy transfer and obtained the apparent diffusion coefficient values by making rather severe assumptions about f_m. In addition, we carried out mathematical simulations of diffusion satisfying Fick's law in a spherical geometry, taking into account the gel content of the particles. The concentration profiles of donor and acceptor groups, which follow the segment density profile of the polymer, were introduced into equations describing the rate of FRET in spherical systems, and the donor decay profiles were simulated. By comparing simulated and experimental decay profiles as a function of annealing time and temperature, the concentration profiles across the interface and corresponding mean cumulative diffusion coefficients $\langle D\rangle$ were obtained. This model can be used to describe the effect of diffusion on FRET in different samples containing a diffusive component and an immobile fraction.

The mean cumulative diffusion coefficient $\langle D\rangle$ was found to decrease with annealing time as a result of the polymer polydispersity and possibly initial rapid interdigitation of the chain ends of highly branched/cross-linked chains that are anchored to the gel network. We also noticed that the mixing between polymer from different particles taking place before annealing is much

lower for gel containing latex particles than that found for un-cross-linked samples.

A comparison of the two different methods showed that D_{app} values are up to three times larger than $\langle D \rangle$, but track the evolution of $\langle D \rangle$ fairly well for the level of precision usually needed in these experiments. From the temperature dependence of the diffusion coefficients, we found an effective activation energy for diffusion of $E_a = 37$ kcal/mol for D_{app} and 39 kcal/mol for $\langle D \rangle$, which are also in good agreement with the value obtained by rheology measurements on the same sample.[26] We conclude that, despite its severe assumptions, the simplified approach, where we calculate f_m values from the quantum efficiency of energy transfer, can track the effect of temperature on diffusion for gel-containing-latex film formation. These results extend the range of application of the simplified model, which had been previously tested for un-cross-linked and unbranched latex particles, both experimentally[23] and by simulation.[29]

Acknowledgment. The authors thank ICI Paints, National Starch, and NSERC for their support of this research and thank Dr. J. P. Tomba and Prof. J. M. G. Martinho for valuable discussions. J.P.S.F. acknowledges financial support from FCT and FEDER (POCTI/QUI/47885).

References and Notes

(1) Kausch, H. H.; Tirrell, M. *Annu. Rev. Mater. Sci.* **1989**, *19*, 341.
(2) Tirrell, M. *Rubber Chem. Technol.* **1984**, *57*, 523.
(3) Spiro, J. G.; Farinha, J. P. S.; Winnik, M. A. *Macromolecules* **2003**, *36*, 7791.
(4) Shearmur, T. E.; Clough, A. S.; Drew, D. W.; van der Grinten, M. G. D.; *Macromolecules* **1996**, *29*, 7269.
(5) Eduards, S. F.; Doi, M. *The Theory of Polymer Dynamics*; Oxford University Press: Oxford, England, 1988.
(6) de Gennes, P. G. *Scaling Concepts in Polymer Physics*, Cornell University Press: Ithaca, NY, 1979.
(7) Zhang, H.; Wool, R. P. *Polym. Prepr.* **1990**, *2*, 511; *Macromolecules* **1989**, *22*, 3018.
(8) Wool, R. P. *Polymer Interfaces: Structure and Strength*, Carl Hanser Verlag: Munich, 1995.
(9) Vanderhoff, J. W. *Br. Polym. J.* **1970**, *2*, 161.
(10) Kanig, G.; Neff, H. *Colloid Polym. Sci.* **1975**, *253*, 29. Distler, D.; Kanig, G. *Colloid Polym. Sci.* **1978**, *256*, 1052.
(11) Roulstone, B. J.; Wilkinson, M. C.; Hearn, J.; Wilson, A. J. *Polym. Int.* **1991**, *24*, 87.
(12) Wang, Y.; Kats, A.; Juhu, D.; Winnik, M. A.; Shivers, R. R.; Dinsdale, C. J. *Langmuir* **1992**, *8*, 1435. Wang, Y.; Winnik, M. A. *J. Phys. Chem.* **1993**, *97*, 2507.
(13) Eckersley, S. T.; Rudin, A. *J. Paint. Technol.* **1990**, *62*, 89.
(14) Joanicot, M.; Wong, K.; Marquet, J.; Chevalier, Y.; Pichot, C.; Graillat, C.; Lindner, P.; Rios, L.; Cabane, B. *Prog. Colloid Polym. Sci.* **1990**, *81*, 157. Chevalier , Y.; Pichot, C.; Graillat, C.; Janicot, M.; Wong, K.; Lindner, P.; Cabane, B. *Colloid Polym. Sci.* **1992**, *270*, 806.
(15) Hahn, K.; Ley, G.; Schuller, H.; Oberthur, R. *Colloid Polym. Sci.* **1986**, *264*, 1029; **1988**, *266*, 631.
(16) Linne, M. A.; Klein, A.; Sperling, L. H. *J. Macromol. Sci. Phys.* **1988**, B27, *181*, 217. Yoo, J. N.; Sperling, L. H.; Glinka, C. J.; Klein, A. *Macromolecules* **1990**, *23*, 3962.
(17) Förster, T. *Ann. Phys. (Leipzig)* **1948**, *2*, 55.
(18) Lakowicz, J. R. *Principles of Fluorescence Spectroscopy*; Plenum Press: New York, 1983.
(19) Farinha, J. P. S.; Martinho, J. M. G.; Kawaguchi, S.; Yekta, A.; Winnik, M. A. *Macromolecules* **1995**, *28*, 6084.
(20) Winnik, M. A.; Pinenq, P.; Krüger, C.; Zhang, J.; Yaneff, P. V. *J. Coat. Technol.* **1999**, *71*, 47.
(21) Zhao, C. L. Wang, Y.; Hruska, Z.; Winnik, M. A. *Macromolecules* **1990**, *23*, 4082.
(22) Kim, H.; Winnik, M. A. *Macromolecules* **1995**, *28*, 2033.
(23) Ye, X. D.; Farinha, J. P. S.; Oh, J. K. Winnik, M. A. Wu, C. *Macromolecules* **2003**, *36*, 8749.
(24) Britton, D.; Heatley, F.; Lovell, P. A. *Macromolecules* **1998**, *31*, 2828.
(25) Wu, J.; Oh, J. K.; Yang, J.; Winnik, M. A.; Farwaha, R.; Rademacher, J. *Macromolecules* **2003**, *36*, 8139.
(26) Wu, J.; Tomba, J. P.; Winnik, M. A.; Farwaha, R.; Rademacher, J. *Macromolecules* **2004**, *37*, 2299.
(27) Wu, J.; Tomba, J. P.; Winnik, M. A.; Farwaha, R.; Rademacher, J. *Macromolecules* **2004**, *37*, 4247.
(28) O′Connor, D. V.; Phillips, D. *Time-Correlated Single Photon Counting*; Academic Press: London, 1984.
(29) Farinha, J.; Martinho, J. M. G.; Yekta, A.; Winnik, M. A. *Macromolecules* **1995**, *28*, 6084.
(30) Dhinojwala, A.; Torkelson, J. M. *Macromolecules* **1994**, *27*, 4817.
(31) Liu, Y. S.; Feng, J. R.; Winnik, M. A. *J. Chem. Phys.* **1994**, *101*, 9096.
(32) Kim, H. B.; Winnik, M. A. *Macromolecules* **1994**, *27*, 1007.
(33) Kim, H. B.; Winnik, M. A. *Macromolecules* **1995**, *28*, 2033.
(34) Crank, J. *The Mathematics of Diffusion*; Clarendon: Oxford, England, 1974.
(35) Yekta, A.; Winnik, M. A.; Farinha, J. P. S.; Martinho, J. M. G. *J. Phys. Chem. A* **1997**, *101*, 1787.
(36) Martinho, J. M. G.; Farinha, J. P. S.; Berberan-Santos, M. N.; Duhamel, J.; Winnik, M. A. *J. Chem. Phys.* **1992**, *96*, 8143.
(37) Förster, T. *Ann. Phys. (Leipzig)* **1948**, *2*, 55; *Z. Naturforsch.* **1949**, *4a*, 321.
(38) Baumann, J.; Fayer, M. D. *J. Chem. Phys.* **1986**, *85*, 4087.
(39) Lakowicz, J. R. *Principles of Fluorescence Spectroscopy*, 2nd ed.; Plenum: New York, 1999.
(40) Bevington, P. R. *Data Reduction and Error Analysis in the Physical Sciences*, McGraw-Hill: New York, 1969.
(41) Farinha, J. P. S.; Martinho, J. M. G.; Xu, H.; Winnik, M. A.; Quirk, R. P. *J. Polym. Sci., Part B: Polym. Phys.* **1994**, *321*, 635.
(42) Winnik, M. A.; Li, L.; Liu, Y. S.; In *Microchemistry: Spectroscopy and Chemistry in Small Domains*; Masuhara H., Kitamura, N., Eds.;Elsevier: Amsterdam, 1994; p 389.
(43) Winnik, M. A.; Liu, Y. S. *Makromol. Chem. Makromol. Symp.* **1995**, *92*, 321.
(44) Geoghegan, M.; Bou, F.; Bacri, G.; Menelle, A.; Bucknall, D. G. *Eur. Phys. J. B* **1998**, *3*, 83.
(45) Ferry, J. D. *Viscoelastic Properties of Polymers*, 3rd ed.; Wiley: New York, 1980.
(46) Wang, Y. C.; Winnik, M. A. *J. Phys. Chem.* **1993**, *97*, 2507.
(47) Antonietti, M.; Sillescu, H. *Macromolecules* **1985**, *18*, 1162.
(48) Lyness, J. N. *SIAM Review* **1983**, *25*, 63.
(49) Although this value is determined for the dispersion, we expect that upon film formation (before interdiffusion) the particles are deformed but their size is not altered.
(50) Farinha, J. P. S.; Martinho, J. M. G.; Pogliani, L. *J. Math. Chem.* **1997**, *21*, 131.
(51) Farinha, J. P. S.; Vorobyova, O.; Winnik, M. A. *Macromolecules* **2000**, *33*, 5863.
(52) Farinha, J. P. S.; Martinho, J. M. G.; Charreyre, M.-T.; Pichot, C.; Winnik, M. A. *Langmuir* **2001**, *17*, 2617.
(53) Geoghegan, M.; Clarke, C. J.; Boue, F.; Menelle, A.; Russ, T.; Bucknall, D. G. *Macromolecules* **1999**, *32*, 5106.

MA050167I